Magnetic Resonance Imaging 92 (2022) 180–186

Contents lists available at ScienceDirect

Magnetic Resonance Imaging

journal homepage: www.elsevier.com/locate/mri

Universal pulses for homogeneous excitation using single channel coils

Ronald Mooiweer [a,b,c], Ian A. Clark [d], Eleanor A. Maguire [d], Martina F. Callaghan [d], Joseph V. Hajnal [a,b], Shaihan J. Malik [a,b,*]

[a] School of Biomedical Engineering and Imaging Sciences, Faculty of Life Sciences and Medicine, King's College London, London, United Kingdom
[b] Center for the Developing Brain, School of Biomedical Engineering and Imaging Sciences, King's College London, St. Thomas' Hospital, London, United Kingdom
[c] MR Research Collaborations, Siemens Healthcare Limited, Camberley, United Kingdom
[d] Wellcome Centre for Human Neuroimaging, UCL Queen Square Institute of Neurology, University College London, London, United Kingdom

ARTICLE INFO

Keywords:
Single channel excitation
Universal pulse
Neuroimaging
SPINS

ABSTRACT

Purpose: Universal Pulses (UPs) are excitation pulses that reduce the flip angle inhomogeneity in high field MRI systems without subject-specific optimization, originally developed for parallel transmit (PTX) systems at 7 T. We investigated the potential benefits of UPs for single channel (SC) transmit systems at 3 T, which are widely used for clinical and research imaging, and for which flip angle inhomogeneity can still be problematic.

Methods: SC-UPs were designed using a spiral nonselective k-space trajectory for brain imaging at 3 T using transmit field maps (B_1^+) and off-resonance maps (B_0) acquired on two different scanner types: a 'standard' single channel transmit system and a system with a PTX body coil.

The effect of training group size was investigated using data (200 subjects) from the standard system. The PTX system was used to compare SC-UPs to PTX-UPs (15 subjects). In two additional subjects, prospective imaging using SC-UP was studied.

Results: Average flip angle homogeneity error fell from 9.5 ± 0.5 % for 'default' excitation to 3.0 ± 0.6 % using SC-UPs trained over 50 subjects. Performance of the UPs was found to steadily improve as training group size increased, but stabilized after ~15 subjects.

On the PTX-enabled system, SC-UPs again outperformed default excitation in simulations (4.8 ± 0.6 % error versus 10.6 ± 0.8 % respectively) though greater homogenization could be achieved with PTX-UPs (3.9 ± 0.6 %) and personalized pulses (SC-PP 3.6 ± 1.0 %, PTX-PP 2.9 ± 0.6 %).

MP-RAGE imaging using SC-UP resulted in greater separation between grey and white matter signal intensities than default excitation.

Conclusions: SC-UPs can improve excitation homogeneity in standard 3 T systems without further calibration and could be used instead of a default excitation pulse for nonselective neuroimaging at 3 T.

1. Introduction

Inhomogeneity of the radio frequency transmit field (B_1^+) reduces the quality of images obtained at main magnetic field strengths of 3 T and higher [1,2]. B_1^+-mitigating techniques have predominantly been developed for Ultra High Field (7 T and higher), involving parallel transmission (PTX), radio frequency pulse design and combinations of both [3]. These techniques are often based on subject-specific, measured, field distributions and thus require some time and effort to tailor the solution to the subject in the scanner. Recently however, the universal pulse (UP) approach has been introduced [4], which exploits similarity in field distributions across subjects. UPs were calculated based on the field maps of a training group of subjects, after which they could be applied to other subjects to retrieve the excitation homogeneity. In general, UPs yield better homogeneity than standard RF pulses but do not achieve the same performance as fully subject-specific pulses. This drawback is offset by avoiding spending time on acquiring field maps and doing calculations for every individual subject, making UPs suitable for standard clinical workflow.

UPs were originally considered for PTX coils at 7 T [4] and have been extended from T1 weighted imaging to 3D Turbo Spin Echo sequences [5] and gradient echo EPI [6]. 'Universal' (i.e. group optimized)

* Corresponding author at: School of Biomedical Engineering and Imaging Sciences, King's College London, 1st Floor South Wing, St Thomas' Hospital, Westminster Bridge Road, London SE1 7EH, United Kingdom.
E-mail address: shaihan.malik@kcl.ac.uk (S.J. Malik).

https://doi.org/10.1016/j.mri.2022.07.002
Received 22 December 2021; Received in revised form 24 June 2022; Accepted 7 July 2022
Available online 9 July 2022

solutions have also been shown to improve performance for the Direct Signal Control (dynamic RF shimming) PTX method applied to 3D FLAIR imaging at 7 T [7] and for body imaging at 3 T [8] and 7 T [9]. While not as severe as at 7 T, B_1^+ inhomogeneity is also still an issue for 3 T neuroimaging both for quantitative methods and structural imaging requiring automated segmentation. The objective of the work reported here is to introduce calibration-free universal pulses for homogeneous excitation within T1 weighted sequences for neuroimaging at 3 T using standard clinical systems that use single channel (SC) excitation. Important questions to be addressed before UPs can be applied widely with confidence are the minimal training group size needed, and the performance on a large range of subjects. Previous studies with UPs showed marked improvement compared to default excitation, often using relatively small (6–20) sample sizes for training [4,5,10,11].

In this study, universal pulses were designed and evaluated on a large set of field maps that were acquired as part of a larger neuroscience study [12,13] using standard 3 T scanners, where B_1^+ maps were used to correct quantitative MRI maps. Although most previous work on UPs used adaptations of k_T-points RF pulse design [14], this work used the spiral nonselective excitation (SPINS) trajectory which has already been shown to reduce excitation inhomogeneity at 3 T both using PTX and SC excitation [15]. A prototype PTX-capable 3 T scanner was also used to investigate differences in performance between SC-UPs and PTX-UPs, and to perform a prospective imaging demonstration on two subjects. Aspects of this study were presented at the annual meeting of the ISMRM in 2017 [16].

2. Methods

2.1. UP design using SPINS

SPINS pulse design uses the spatial domain method [17] which may be written as a matrix problem.

$$\mathbf{m} = \mathbf{A}\,\mathbf{b}, \tag{1}$$

where **m** is the target magnetization in the subject, ***A*** is a system matrix constructed based on the subject's B_1^+ and B_0 field maps, the spatial coordinates of the voxels, and the prescribed 3D non-selective k-space trajectory. Lastly, **b** is the complex RF pulse to be determined.

Throughout this work we used a k-space trajectory similar to the one originally proposed in ref. [15] (k_{max} 50 rad/m, u = 12π rad/ms, v = 2π rad/ms, α = 10, β =0.6), with an overall duration of 1.37 ms (0.37 ms gradient-only lead-in and 1 ms with jointly activated RF). Gradient system imperfections were modelled using a gradient impulse response function (GIRF) [18] which was measured using an image-based method similar to that of Papadakis et al. [19]. To find the RF pulses that excite a spatially uniform target magnetization **m, b** is optimized using a magnitude least-squares approach [20]:

$$\boldsymbol{b} = argmin_b \left\{ \| |\boldsymbol{A}\boldsymbol{b}| - \boldsymbol{m} \|^2 + \lambda \|\boldsymbol{b}\|^2 \right\}, \tag{2}$$

where λ is a Tikhonov regularization factor.

To construct a *Universal* SPINS pulse from a training group of N subjects, a combined matrix description of the problem is constructed by concatenating the individual matrices:

$$\begin{bmatrix} \boldsymbol{m_1} \\ \vdots \\ \boldsymbol{m_N} \end{bmatrix} = \begin{bmatrix} \boldsymbol{A_1} \\ \vdots \\ \boldsymbol{A_N} \end{bmatrix} \boldsymbol{b_U}\,, \tag{3}$$

$$\boldsymbol{m_U} = \boldsymbol{A_U}\boldsymbol{b_U}$$

This is then solved using the same magnitude least-squares algorithm to yield a single universal RF pulse waveform $\mathbf{b_U}$. The Tikhonov regularization factor was set to scale with the number of transmit channels and number of subjects in the training group, to reflect the increasing dimensions of the design problem.

2.2. Design considerations of UPs: simulation study

Two-hundred healthy volunteers were included in the study. They were aged between 20 and 41 years old (mean age 28.7 years, standard deviation = 5.6 years), and reported no psychological, psychiatric, neurological or behavioural health conditions. The subjects were scanned over two years and included 98 males and 102 females. The B_1^+ and B_0 maps were collected as part of larger study study [12,13] for which subjects were reimbursed £10 per hour for taking part. All subjects gave written informed consent and the study was approved by the University College London Research Ethics Committee.

These data were collected using three identical 3 T scanners using SC RF transmission (Tim Trio, Siemens Healthcare, Erlangen, Germany), so the data could be pooled without distinguishing between the scanners. In all subjects, the prescribed field of view was the same and no instructions were given to the subjects regarding tilting of the head in the sagittal plane.

B_1^+ maps were acquired using a stimulated echo/spin echo sequence with a 3D EPI read-out [21]. EPI-related distortions were corrected using acquired B_0 maps [2,22]. The FSL-BET brain extraction tool [23] was used to define a region of interest (i.e. the whole brain) in the field maps that was then used for pulse design. For pulse design and subsequent simulations, the maps were down-sampled to a grid of 32 × 32 × 32 voxels (8 × 6 × 6 mm^3).

Universal SPINS pulses were calculated as described in the previous section, using the B_1^+ and B_0 maps of a number of subjects in a training group, and evaluated on a test group using Bloch Equation Simulations [24]. One-hundred subjects were randomly chosen as the test group on which UPs with various design parameters were evaluated. This test group was fixed across all simulations to facilitate a consistent comparison between design methods. The effect of the training group size ($N_{training}$) on the efficacy of UPs was evaluated using simulation. In each case, UPs were designed using B_1^+ and B_0 maps from $N_{training}$ subjects randomly selected from the 100 not included in the test group. This process was repeated 20 times for each value of $N_{training}$ to avoid selection bias and to study the variability/stability with respect to the random selection of training subjects, always evaluated on the same testing group.

A possible improvement to the design of universal SPINS pulses was considered, addressing natural variation in the positioning of a subject's head in the scanner. Under the assumption that both B_1^+ and B_0 distributions are fixed with respect to the head, relative head position can be accounted for by shifting the measured B_1^+ and B_0 distributions. Based on this assumption we attempted to make the SC-UP more effective by applying a phase correction term $\phi(t) = \boldsymbol{k}(t).\,\boldsymbol{\Delta r}$ to the RF pulse based on an individual's head position within the coil, with $\boldsymbol{\Delta r}$ the vector of the brain center of mass from the origin of the coordinate system, determined from a mask of the brain. When using this method, UPs were calculated after first centering the coordinate system for each training dataset (i.e. by setting $\boldsymbol{\Delta r} = \mathbf{0}$ for each subject). This is possible because in the concatenated UP design approach (Eq. [3]) each subject has their own system matrix **A** which contains the coordinate system within it.

2.3. Comparison of SC and PTX UPs: simulation study

A different 3 T scanner (Achieva, Philips Medical Systems, Best, The Netherlands) with an eight-channel PTX body coil [25] was used to compare SC and PTX performance in UPs. The quadrature mode of this system ('single-channel mode') is similar to that of a whole body birdcage coil [25]. By either designing pulses for the individual channels or the combination of channels driven in quadrature mode, a direct comparison of UPs for PTX and SC body coils could be made. One of the transmit channels was excluded from all experiments (including SC mode) due to a technical failure, resulting in a system capable of 7-channel PTX. An eight-channel head coil was used throughout for signal reception.

For the comparative simulation study, field maps were acquired in 15 healthy volunteers (9 male, 6 female). They were aged between 23 and 35 years old (mean age 28.8 years, standard deviation = 3.7 years). All subjects gave written informed consent and the study was approved by London Riverside Research Ethics Committee. Multi-channel B_1^+ maps were acquired using an interferometric approach [26,27] with a combination of low flip angle spoiled gradient echo (SPGR) (nominal flip angle 1°, TR = 3.5 ms, TE = 1.5 ms) for each linear combination of channels, and a single 3D actual flip angle imaging (AFI) [28] map (nominal flip angle 80°, TR = 30, 150 ms, TE = 4.6 ms) in quadrature mode. The SPGR images were used to compute relative B_1^+ and the AFI map scales to the correct absolute level – a similar approach was used in refs [29, 30]. B_0 maps were acquired using dual echo SPGR (ΔTE = 2.3 ms). Field maps were acquired at isotropic resolution 3.91 × 3.91 × 3.91 mm^3 and down sampled to a matrix size 32 × 32 × 32 (8 × 8 × 8 mm^3). For each subject, the FSL-BET brain extraction tool [23] was used to define the whole brain as region of interest for pulse design.

Universal pulse simulations were carried out using a leave-one-out method: UPs were calculated using the field maps of 14 subjects and evaluated on the remaining subject, this was then repeated for every subject. Personalized pulses (PP) were also designed for SC and PTX operation of the body coil using the conventional SPINS method.

2.4. Data analysis: ε = pre-normalized NRMSE

To compare the homogeneity of the different excitation strategies, a figure of merit ε was defined as the normalized root mean square error of the normalized simulated excitation profile over the brain (equivalent to the coefficient of variation). In this way, ε only reflected the variation in flip angle per subject, it could be compared across different subjects, but it did not take in account overall offsets in flip angle. Flip angle offsets might be corrected in practice by amplitude scaling of the RF pulses, as is commonly done for conventional RF excitation (transmitter gain adjustment).

2.5. MP-RAGE imaging with SC-UP: imaging study

The same PTX-enabled system was also used to demonstrate SC-UPs in MP-RAGE imaging of two additional healthy volunteers (1 male, 1 female, aged 25 and 27 years old) who gave written informed consent for this study that was approved by the London Riverside Research Ethics Committee. The Alzheimer's Disease Neuroimaging Initiative MP-RAGE protocol [31] was used with both standard RF pulses, and after replacing the small flip angle excitation pulses (flip angle 8°) with UPs. In all cases the inversion pulse was a adiabatic hyperbolic secant pulse and the other scan parameters were: shot TR = 3000 ms, shot AQ duration = 1800 ms, min. TI delay = 936 ms, shots = 182, TE = 3.2 ms, TR = 7.5 ms, $N_{TR\ per\ shot}$: 240, BW 241 Hz, FOV = 256 × 240 × 170 mm^3 (FH x AP x RL), matrix = 256 × 240, slices = 142, voxel size: 1.0 × 1.0 × 1.2 mm^3, scan duration = 9m5s.

The SC-UP was calculated from field maps of the 15 subjects scanned on this system. As previous work has shown that tailored RF pulses at flip angle 8° can improve excitation homogeneity but not contrast [15], MP-RAGE imaging was also performed with SC-UP at a flip angle of 5.5°, the effective flip angle that is achieved in the cortex with quadrature mode excitation. The images were first brain extracted and then bias

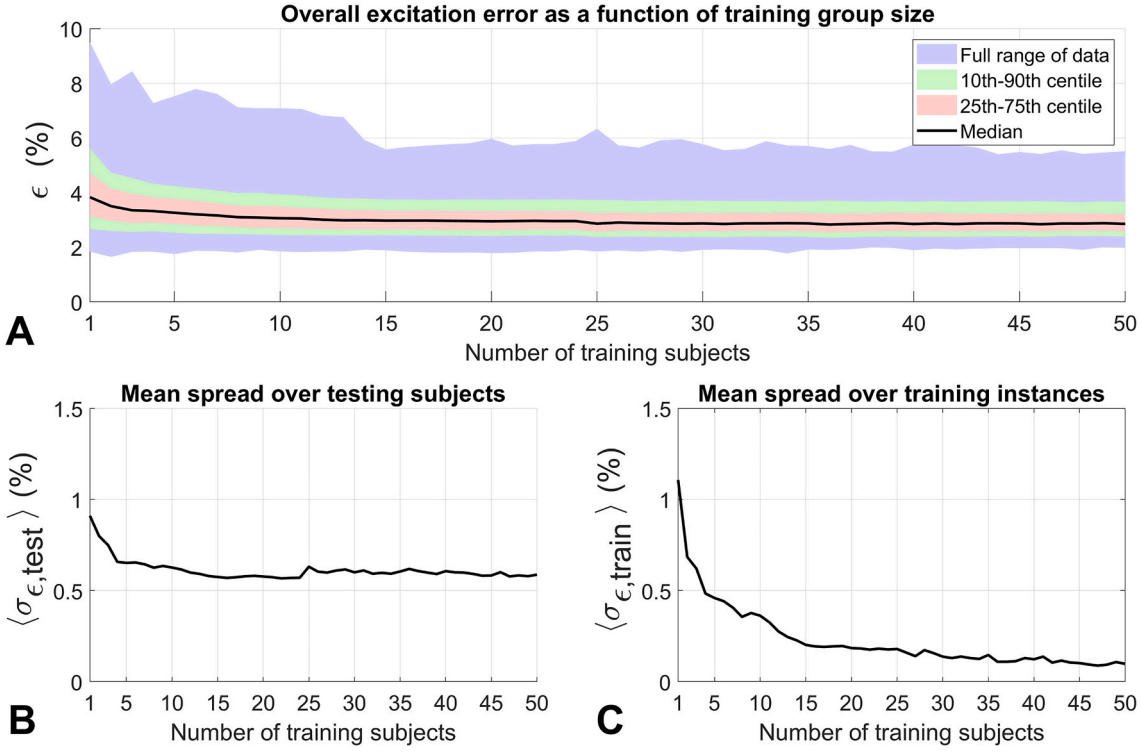

Fig. 1. A) Simulated excitation homogeneity errors ε of SC-UPs optimized using 1–50 training subjects, evaluated on 100 testing subjects, and repeated 20 times with different selections of training subjects. Although the total spread in ε per experiment with a fixed training group size is 4 percentage point or larger, the majority of the simulations are within a much narrower range of ~1 percentage point in ε. **B)** Mean over training group instantiations, of the standard deviation across the 100 testing subjects of ε of the simulated SC-UP excitation evaluated: $\langle \sigma_{\varepsilon,\ test} \rangle$. Aside from the very smallest training group size, the standard deviation is generally constant, reflecting the variation in test subjects' field maps and the resulting excitation errors over the test subjects. These remain around 0.6 percentage point no matter how much data is included in the training group size. **C)** Mean across all test subjects, of the standard deviation across the 20 independent training instances of the same training group size of ε of the simulated SC-UP excitation: $\langle \sigma_{\varepsilon,\ train} \rangle$.The variable resulting ε as a function of selecting different training subjects drops rapidly until ~15 training subjects, after which ε reduces very gradually with increasing training group size. This suggests that once a training group size of 15 is reached, the results of SC-UPs are largely independent of which specific subjects are used for training.

field corrected using FSL FAST [32].

3. Results

3.1. Design considerations of UPs: simulation study

The results of varying the training group size are summarized in Fig. 1A, where every entry in the graph is based on the simulated performance on 100 test subjects, repeated 20 times for different selections of the training group. Remarkably, even for a training group size of 1 the mean ε of the SC-UP (4.0 ± 1.2 %) is far below that of default excitation (9.5 ± 0.5 %). Increasing the group size brings down the average ε: 3.1 ± 0.6 % for $N_{training} = 15$ and 3.0 ± 0.6 % for $N_{training} = 50$. When any 15 or more subjects are chosen, the worst ε over all test subjects is below 6.5%, and 80% of the simulations are within ~1% of the average value of ε. Fig. 1B shows the standard deviation of ε across the 100 different testing subjects, averaged over the 20 different instances of training group. It shows that a spread of ~0.6% is present for any training group size (5–50) in these experiments, due to the differences in properties of the 100 testing subjects. In contrast, in Fig. 1C, the average standard deviation across repetitions of the training instances decreased with an increasing number of training subjects. Low values here (~0.2% for 15–20 subjects) show that the performance of the UP is stable no matter which training subjects are chosen as long as there are a sufficient number. The best results were obtained with 50 subjects inside the training group, but the improvement is small compared to $N_{training} = 15$.

Possible improvements of brain centering are shown for a 'stable' training group size of 15 in Fig. 2. This demonstrates that, even though a modest average improvement was obtained by using brain centering in UPs, not all subjects benefitted from this method.

In Fig. 3 the performance of SC-UPs ($N_{training} = 15$, brain centering enabled) was compared to default excitation and personalized single channel SPINS pulses (SC-PP). Tailored pulses performed best, with a small spread, but SC-UPs also provided a large improvement versus the default excitation, and performed better than default excitation in all cases.

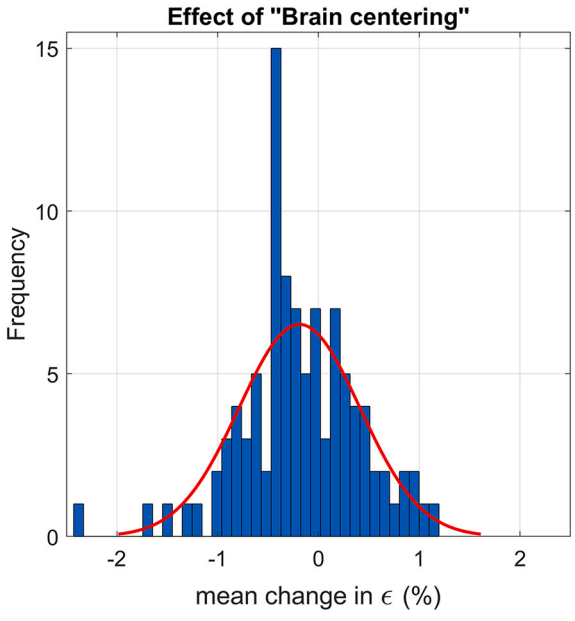

Fig. 2. Change in ε caused by "brain centering"; histogram plots the distribution over test subjects, in each case averaged over all training instances. The red line shows a fitted Gaussian distribution, with mean -0.19 and standard deviation 0.60 percentage units. There is a small average 'improvement' from brain centering, in that the average change in ε is negative, however the improvement is small compared with the variability over test subjects. (For interpretation of the references to colour in this figure legend, the reader is referred to the web version of this article.)

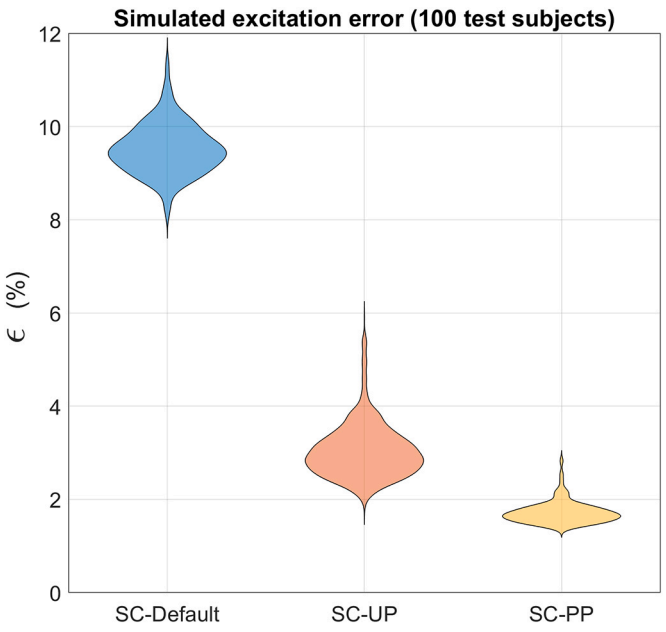

Fig. 3. Distributions of simulated ε values for single channel excitation using the default non-selective pulse, SC-UP (Ntraining = 15, brain centering enabled, repeated 20 times with new selection of training subjects), and SC-PP (personalized SPINS pulse). There is no overlap between the distributions of default excitation and SC-UP, indicating that SC-UPs always outperformed defualt excitation in terms of ε. Mean and standard deviations are: default 9.5 ±0.5, SC-UP 3.0±0.6, SC-PP 1.7±0.2.

3.2. Comparison of SC and PTX UPs: simulation study

In the simulations for the PTX-enabled system, the SC-UP again performed consistently better than the default quadrature mode (Fig. 4), reducing the mean ε from 10.6 ± 0.8 % to 4.8 ± 0.6 %. Personalized designs (SC-PP, PTX-PP) and using PTX for UP design tended to reduce the excitation error somewhat further (3.6 ± 1.0 %, 2.9 ± 0.6 % and 3.9 ± 0.6 %, respectively), as expected.

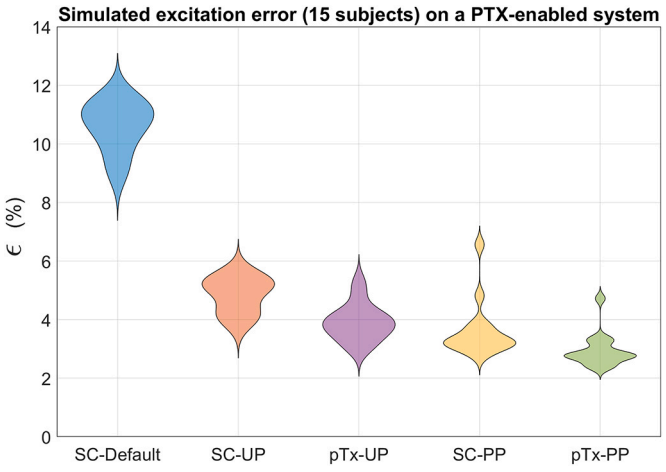

Fig. 4. Excitation variations simulated for the PTX-enabled 3 T scanner in 15 subjects using default, SC-UP, PTX-UP, SC-PP, and PTX-PP. SC-UPs always resulted in lower excitation error than default excitation. Additional reductions were achieved by using PTX and PP.

3.3. MP-RAGE imaging with SC-UP: imaging study

The SC-UP, calculated using the field maps of all 15 previously-acquired datasets on the PTX system, is shown in Fig. 5. Post-bias field correction MP-RAGE images for 1 volunteer are shown in Fig. 6. The contrast in the image acquired with SC-UP at 8° flip angle didn't improve compared to default excitation: although a greater excitation homogeneity can be expected by the use of UP, the 8° flip angle is known to generate insufficient contrast in MP-RAGE images. However, the MP-RAGE image acquired with SC-UP at 5.5° flip angle does display better contrast, also demonstrated by a larger separation between the white matter and grey matter peaks in the histograms of both volunteers (Fig. 7).

4. Discussion

This paper investigated the use of a universal pulse for homogeneity correction of 3 T brain imaging with body coil excitation. Simulations using a large set of field map data acquired from 200 subjects (100 used for testing) showed that SC-UP outperformed standard quadrature excitation, achieving an average ε of 3.1 ± 0.3 % with 15 training subjects, compared to 9.5 ± 0.5 % with default SC excitation in simulation. A training group size of 15 is recommended as this number marked a drop in the spread in the variability of the simulated results. For both individuals in the acquired imaging experiments and in all simulations (with a large enough training group size) the excitation performance for the UP was never worsened in the test subjects.

When used prospectively for MP-RAGE imaging, SC-UPs yielded good image quality and clearly showed improved tissue contrast. As in the original publication on SPINS [15], it was found that improved contrast for the cortex could only be achieved after reducing the target flip angle. This can be explained by the fact that when using 'default' excitation pulses, the flip angle that is actually achieved in the cortex is much lower than the specified value. Consequently, if this excitation is made uniform, a higher flip angle (with lower contrast) is actually achieved there. Similar behaviour was observed in the present study, with the signal histograms in Fig. 7 confirming that the 5.5° SC-UP yielded the greatest difference between grey and white matter peaks.

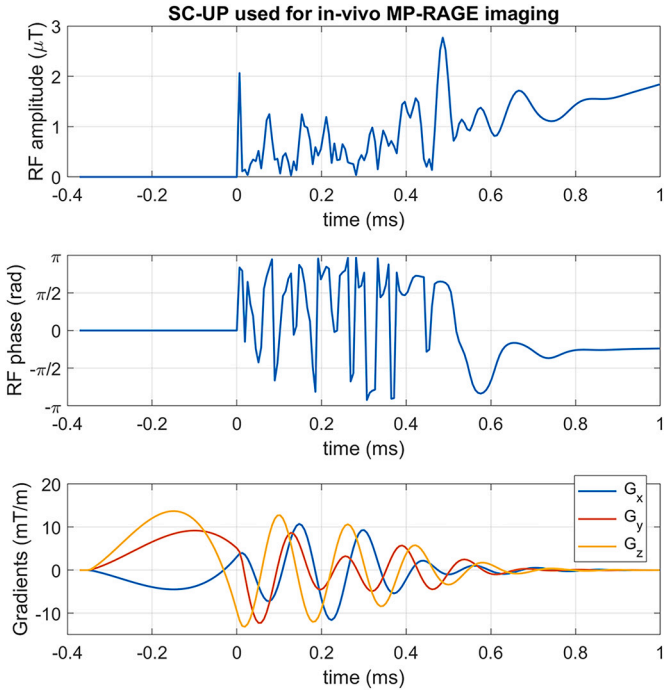

Fig. 5. RF and gradient waveforms of the single channel universal SPINS pulse (SC-UP), optimized using 15 training subjects, which was used for MP-RAGE imaging in 2 different healthy volunteers. RF amplitude was scaled to provide a 5.5° excitation. The gradient waveforms shown are the desired waveforms, before pre-emphasis for the system response using the measured GIRF.

In the simulation experiments presented here, ε on average was reduced from 9.5 ± 0.5 % to 3.0 ± 0.6 % with UPs while personalized pulses could reach 1.7 ± 0.2 %. These results replicate the trend of the original UP work, which reported normalized root mean square errors of ~28, ~11 and ~ 7% respectively [4]. In our work ε is reported which only described homogeneity differences and not the overall flip angle offset, which is assumed to be corrected for in practise using subject specific power scaling. Other differences between this and the original UP work include field strength, coil type, RF pulse design method, and inclusion of the training group in the simulation results.

Simulation results from the PTX system were similar to those from the more standard SC 3 T systems, although the error in the 'default' (i.e. quadrature) mode was higher, likely because the PTX system was used with only 7 of the 8 transmit channels due to hardware failure. Nevertheless, we observed the expected hierarchy of performance, with PTX in general outperforming single channel operation, and personalized pulses generally outperforming universal ones. That said, switching from SC-Default to SC-UP yielded the largest drop in ε for both the regular SC scanner and the PTX scanner.

This work did not consider optimizing the k-space trajectory for 'universal' application; instead we used fixed trajectory properties (as reported in methods) which were close to the original SPINS implementation. The universal pulses were designed to be used as small flip angle excitation pulses in an MP-RAGE imaging sequence at 3 T, the application for which the SPINS pulses were originally designed. A similar approach could be attempted for other imaging applications, but in such a case alternative pulse design methods could be investigated. For example, the specific absorption rate (SAR) was not explicitly taken into account in the current work since the small flip angle pulses being designed have very low energy and the total sequence SAR of the MP-RAGE sequence with standard pulses (including adiabatic inversion pulses) is well below the limit (~7% [15]). Such a consideration could be added in the future, particularly if high flip angle pulses are desired. Furthermore, in this work a GIRF was used to map from applied gradients to k-space trajectory for pulse design. In order to compare universal pulses as function of field maps and not of gradient performance, the GIRF measured on the PTX-enabled Philips system was imposed on the pulse design for the SC Siemens system. For widespread application of universal pulses, the calibration for imperfect gradient response may need to be scanner specific and could be obtained using either image based measurements (as done in this work [19]) or field probes [18]; previous work has found these can be used interchangeably [33]. Calibration is not patient specific and may only be needed once per scanner, as the GIRF has been observed to remain stable over long periods of time [15].

An additional hypothesis tested in this work was that the performance of UPs might be improved by accounting for differences in the positioning of the head relative to the scanner. Our results show that although a small benefit was observed from correcting the pulses for head position, it did not improve the results for ~40% of the subjects, and the differences in the large majority of cases were small compared with the variability within the testing group. This may have been because the assumption of invariance of the B_1^+ and B_0 field patterns to the head position is not met in practice. We conclude that there is not a strong case for additional subject-specific calibration for head position, which is a positive outcome in practical terms since it does not complicate the required workflow.

This work addressed B_1^+ inhomogeneity in the brain at 3 T, demonstrating that improvements in image quality are possible with single channel universal pulses. It is well known that B_1^+ variations are stronger for body imaging at this field strength and an automated selection of PTX universal pulses has been shown to mitigate these effects in the

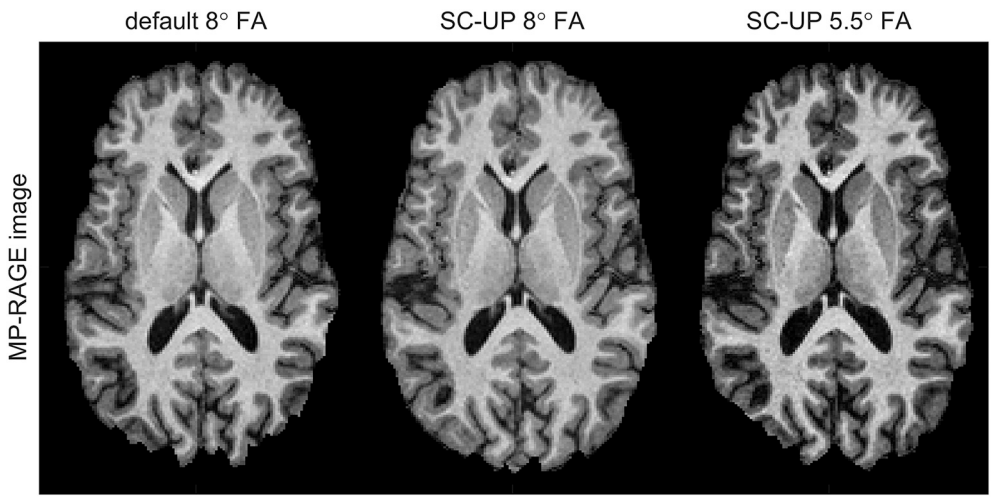

Fig. 6. Bias field corrected MP-RAGE images acquired in one subject using default excitation and SC-UPs at FA 8° and 5.5°.

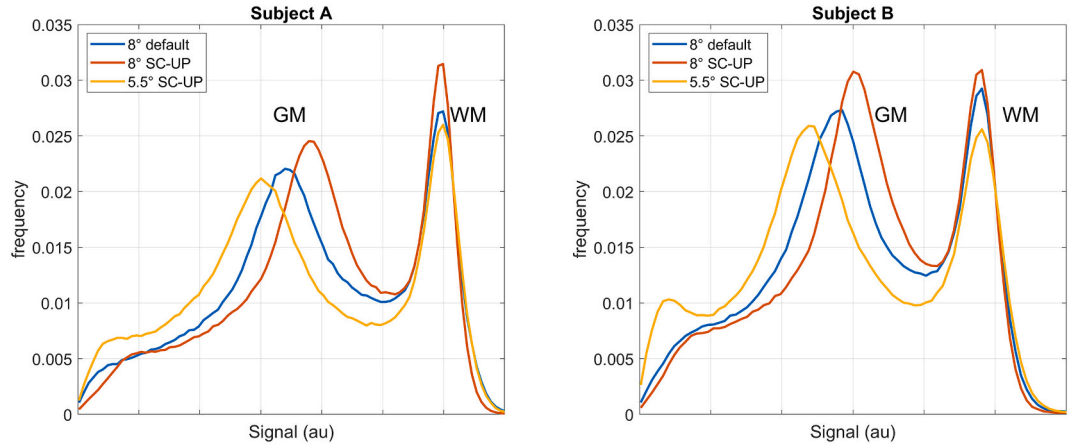

Fig. 7. Signal intensity histograms of MP-RAGE images acquired in two subjects after bias field correction, using default excitation and the SC-UP at flip angles of 8° and 5.5°. Compared to default excitation, using SC-UP at 8° reduced the gap between grey (GM) and white matter (WM). However, when the SC-UP was used at the optimized 5.5° flip angle, the separation between the GM and WM improved.

presence of large morphological variations [8]. Further research is required to determine whether improvements could also be obtained using only single channel transmission for this application.

5. Conclusions

Single Channel Universal Pulses using SPINS have been shown to be suitable for use in low flip angle (GRE) sequences using non-selective excitation to improve excitation homogeneity without spending time on subject-specific pulse design. Given that there is no intrinsic cost to using these methods, and that they may improve data quality and improve the performance of image post-processing methods, SC-UPs could be used on standard 3 T MR systems in clinical and investigational neuroimaging.

Declaration of Competing Interest

Ronald Mooiweer is seconded to Siemens Healthcare Limited.

Acknowledgements

This work was supported by the EPSRC (EP/L00531X/1), Medical Research Council (MR/K006355/1), a Wellcome Principal Research Fellowship to E.A.M. (01759/Z/13/Z), a Wellcome Strategic Award to the Wellcome Centre for Human Neuroimaging (203147/Z/16/Z), Wellcome/EPSRC Centre for Medical Engineering (WT 203148/Z/16/Z), and the National Institute for Health Research (NIHR) Biomedical Research Centre at Guy's and St. Thomas' NHS Foundation Trust and King's College London. We thank Anna Monk, Victoria Hotchin and Gloria Pizzamiglio for assistance with data collection. The views expressed are those of the authors and not necessarily those of the NHS, the NIHR or the Department of Health.

This research was funded in whole, or in part, by the Wellcome Trust [Grant numbers: 01759/Z/13/Z; 210567/Z/18/Z; 203147/Z/16/Z; 203148/Z/16/Z]. For the purpose of Open Access, the authors have applied a CC BY public copyright licence to any Author Accepted Manuscript version arising from this submission.

Data from the 200 volunteers are part of a larger project, the data from which will be made available once the construction of a dedicated data-sharing portal has been finalised. In the meantime, requests for the data can be sent to e.maguire@ucl.ac.uk.

References

[1] Wiesinger F, Van de Moortele P-F, Adriany G, De Zanche N, Ugurbil K, Pruessmann KP. Potential and feasibility of parallel MRI at high field. NMR Biomed 2006;19(3):368–78.

[2] Lutti A, Hutton C, Finsterbusch J, Helms G, Weiskopf N. Optimization and validation of methods for mapping of the radiofrequency transmit field at 3T. Magn Reson Med 2010;64(1):229–38.
[3] Padormo F, Beqiri A, Hajnal JV, Malik SJ. Parallel transmission for ultrahigh-field imaging. NMR Biomed 2016;29(9):1145–61.
[4] Gras V, Vignaud A, Amadon A, Le Bihan D, Boulant N. Universal pulses: a new concept for calibration-free parallel transmission. Magn Reson Med 2017;77(2):635–43.
[5] Gras V, Mauconduit F, Vignaud A, Amadon A, Le Bihan D, Stöcker T, et al. Design of universal parallel-transmit refocusing kT-point pulses and application to 3D T2-weighted imaging at 7T. Magn Reson Med 2018;80(1):53–65.
[6] Gras V, Poser BA, Wu X, Tomi-Tricot R, Boulant N. Optimizing BOLD sensitivity in the 7T human connectome project resting-state fMRI protocol using plug-and-play parallel transmission. NeuroImage 2019;195:1–10.
[7] Beqiri A, Hoogduin H, Sbrizzi A, Hajnal JV, Malik SJ. Whole-brain 3D FLAIR at 7T using direct signal control. Magn Reson Med 2018;80(4):1533–45.
[8] Tomi-Tricot R, Gras V, Thirion B, Mauconduit F, Boulant N, Cherkaoui H, et al. SmartPulse, a machine learning approach for calibration-free dynamic RF shimming: preliminary study in a clinical environment. Magn Reson Med 2019;82:2016–31.
[9] Aigner CS, Dietrich S, Schaeffter T, Schmitter S. Calibration-free pTx of the human heart at 7T via 3D universal pulses. Magn Reson Med 2022;87(1):70–84.
[10] Gras V, Boland M, Vignaud A, Ferrand G, Amadon A, Mauconduit F, et al. Homogeneous non-selective and slice-selective parallel-transmit excitations at 7 tesla with universal pulses: a validation study on two commercial RF coils. PLoS One 2017;12(8):e0183562.
[11] Gras V, Pracht ED, Mauconduit F, Le Bihan D, Stöcker T, Boulant N. Robust nonadiabatic T 2 preparation using universal parallel-transmit k T -point pulses for 3D FLAIR imaging at 7 T. Magn Reson Med 2019;81(5):3202–8.
[12] Clark IA, Monk AM, Hotchin V, Pizzamiglio G, Liefgreen A, Callaghan MF, et al. Does hippocampal volume explain performance differences on hippocampal-dependant tasks? NeuroImage 2020;221:117211.
[13] Clark IA, Callaghan MF, Weiskopf N, Maguire EA. The relationship between hippocampal-dependent task performance and hippocampal grey matter myelination and iron content. Brain Neurosci Adv 2021;5:1–8.
[14] Cloos MA, Boulant N, Luong M, Ferrand G, Giacomini E, Le Bihan D, et al. k_T-points: Short three-dimensional tailored RF pulses for flip-angle homogenization over an extended volume. Magn Reson Med 2012;67(1):72–80.
[15] Malik SJ, Keihaninejad S, Hammers A, Hajnal JV. Tailored excitation in 3D with spiral nonselective (SPINS) RF pulses. Magn Reson Med 2012;67(5):1303–15.
[16] Mooiweer R, Hajnal JV, Malik SJ. A single-channel universal SPINS pulse for calibration-free homogeneous excitation without PTX. Proc Intl Soc Mag Reson Med 2017;25:0390.
[17] Grissom W, Yip C-y, Zhang Z, Stenger VA, Ja Fessler, Noll DC. Spatial domain method for the design of RF pulses in multicoil parallel excitation. Magn Reson Med 2006;56(3):620–9.
[18] Vannesjo SJ, Haeberlin M, Kasper L, Pavan M, Wilm BJ, Barmet C, et al. Gradient system characterization by impulse response measurements with a dynamic field camera. Magn Reson Med 2013;69(2):583–93.
[19] Papadakis NG, Wilkinson AA, Carpenter TA, Hall LD. A general method for measurement of the time integral of variant magnetic field gradients: application to 2D spiral imaging. Magn Reson Imaging 1997;15(5):567–78.
[20] Setsompop K, Wald LL, Alagappan V, Gagoski BA, Adalsteinsson E. Magnitude least squares optimization for parallel radio frequency excitation design demonstrated at 7 tesla with eight channels. Magn Reson Med 2008;59(4):908–15.
[21] Jiru F, Klose U. Fast 3D radiofrequency field mapping using echo-planar imaging. Magn Reson Med 2006;56(6):1375–9.
[22] Lutti A, Stadler J, Josephs O, Windischberger C, Speck O, Bernarding J, et al. Robust and fast whole brain mapping of the RF transmit field B1 at 7T. PLoS One 2012;7(3):1–7.
[23] Smith SM. Fast robust automated brain extraction. Hum Brain Mapp 2002;17(3):143–55.
[24] Hargreaves B. Bloch Equation Simulator. Available from: http://mrsrl.stanford.edu/~brian/blochsim/.
[25] Vernickel P, Röschmann P, Findeklee C, Lüdeke KM, Leussler C, Overweg J, et al. Eight-channel transmit/receive body MRI coil at 3T. Magn Reson Med 2007;58(2):381–9.
[26] Brunner DO, Pruessmann KP. B1 + interferometry for the calibration of RF transmitter arrays. Magn Reson Med 2009;61(6):1480–8.
[27] Malik SJ, Larkman DJ, Hajnal JV. Optimal linear combinations of array elements for B 1 mapping. Magn Reson Med 2009;62(4):902–9.
[28] Yarnykh VL. Actual flip-angle imaging in the pulsed steady state: a method for rapid three-dimensional mapping of the transmitted radiofrequency field. Magn Reson Med 2007;57(1):192–200.
[29] Malik SJ, Beqiri A, Padormo F, Hajnal JV. Direct signal control of the steady-state response of 3D-FSE sequences. Magn Reson Med 2015;73(3):951–63.
[30] Van de Moortele P-F, Snyder C, DelaBarre L, Adriany G, Vaughan T, Ugurbil K. Calibration tools for RF Shim at very high field with multiple element RF coils: from ultra fast local relative phase to Absolute magnitude B1+ mapping. Proc Intl Soc Mag Reson Med 2007;15:1676.
[31] Jack CR, Bernstein MA, Fox NC, Thompson P, Alexander G, Harvey D, et al. The Alzheimer's disease neuroimaging initiative (ADNI): MRI methods. J Magn Reson Imaging 2008;27(4):685–91.
[32] Zhang Y, Brady M, Smith S. Segmentation of brain MR images through a hidden Markov random field model and the expectation-maximization algorithm. IEEE Transactions on Medical Imaging 2001;20(1):45–57.
[33] Çavuşoğlu M, Mooiweer R, Pruessmann KP, Malik SJ. VERSE-guided parallel RF excitations using dynamic field correction. NMR Biomed 2017;30(6):1–13.